

Mechanism and Machine Theory
Dynamic Balance Optimization of a Six-Bar Watt Linkage Using Fully Cartesian Coordinates: A Multi-Objective Approach
--Manuscript Draft--

Manuscript Number:	
Article Type:	Research Paper
Keywords:	Dynamic balancing; Six-bar Watt linkage; Multi-objective optimization; Fully Cartesian coordinates
Corresponding Author:	Claudia N. Sanchez, Dr. Universidad Panamericana - Aguascalientes MEXICO
First Author:	Maria Teres Orvañanos-Guerrero
Order of Authors:	Maria Teres Orvañanos-Guerrero Claudia N. Sanchez, Dr. Luis Eduardo Robles-Jiménez Sara Carolina Gómez-Delgado
Abstract:	Balancing mechanisms requires minimizing both the Shaking Moment and Shaking Force, a complex multi-criteria challenge often tackled using single-objective algorithms. However, these methods face difficulties in navigating competing objectives. In contrast, multi-objective algorithms provide a more efficient and adaptable framework, while Fully Cartesian Coordinates simplifies the balancing equations compared to conventional Cartesian formulations. This study focuses on optimizing the dynamic balance of a six-bar Watt linkage using Fully Cartesian Coordinates, comparing the performance of single-objective optimization methods—such as GA, PS, ES, DE, SRES, and ISRES—with multi-objective algorithms, including NSGA-II, NSGA-III, R-NSGA-II, R-NSGA-III, UNSGA-III, MOEA/D, AGE-MOEA, CTAEA, SMS-EMOA, and RVEA. SMS-EMOA demonstrates superior performance, achieving the highest hypervolume metric within 10.44 minutes of execution. The results indicate that multi-objective algorithms outperform single-objective approaches, offering faster and more diverse optimization solutions. Additionally, this study introduces an analytical method that enables the straightforward identification of removable counterweights, achieving an equally effective balance while minimizing the number of counterweights required.
Opposed Reviewers:	

UNIVERSIDAD



Facultad de
Ingeniería

Aguascalientes, México, February 25, 2025.

P. Flores

Editor-in-Chief of Mechanism and Machine Theory

We are pleased to resubmit our revised manuscript “**Dynamic Balance Optimization of a Six-Bar Watt Linkage Using Fully Cartesian Coordinates: A Multi-Objective Approach**”. We sincerely appreciate the reviewers' valuable comments and suggestions, which have helped us improve the quality of our work. In this revised version, we have carefully addressed all the feedback received.

Our research focuses on optimizing the dynamic balance of a six-bar Watt linkage using Fully Cartesian Coordinates, which simplifies balancing equations compared to traditional approaches. We compare single-objective optimization methods (GA, PS, ES, DE, SRES, and ISRES) with multi-objective algorithms (NSGA-II, NSGA-III, R-NSGA-II, R-NSGA-III, UNSGA-III, MOEA/D, AGE-MOEA, CTAEA, SMS-EMOA, and RVEA), demonstrating the advantages of multi-objective approaches in addressing the trade-off between minimizing Shaking Force and Shaking Moment.

We would be grateful if you could consider our revised manuscript for publication in **Mechanism and Machine Theory**. All authors have contributed to the development and design of this study, and we confirm that the manuscript represents valid and original work that has been thoroughly reviewed and approved by all co-authors.

Thank you for your time and consideration. We look forward to your response.

Yours sincerely,

**Dra. Claudia Nallely Sánchez Gómez,
Research Secretary
Engineering Faculty
Universidad Panamericana campus Aguascalientes**

Responses to comments in our previous version

We submitted our manuscript previously and received some comments. We sincerely appreciate the reviewers who helped us improve the quality of our manuscript. Below, we provide a point-by-point response to each reviewer's concerns.

- 1) Highlights are mandatory for this journal. Please follow "Guide for Authors" available online to revise the list of highlights, since they are too long.**
We have revised the highlights following the guidelines provided in the "Guide for Authors" and ensured that they meet the required length and format.
- 2) Please improve and uniformize the graphical quality of the figures used in the manuscript.**
The figures have been updated to enhance their graphical quality and ensure uniformity in style and resolution across the manuscript.
- 3) The English language used throughout the manuscript is rough at some places.**
We have carefully revised the manuscript to improve its language and readability. We also use Grammarly to verify the grammar and improve its readability. In addition, thorough proofreading has been conducted to ensure clarity and correctness.
- 4) There must be no references to websites: they are not permitted in any form whatsoever.**
All references to websites have been removed from the manuscript.
- 5) Please follow "Guide for Authors" to revise and prepare the list of references in a uniform manner.**
The reference list has been reformatted according to the "Guide for Authors," ensuring uniformity and adherence to the journal's required citation style.

We appreciate the opportunity to revise our manuscript and hope that the revised version meets the expectations of the reviewers and the editorial board. Thank you for your time and consideration.

Highlights

Dynamic Balance Optimization of a Six-Bar Watt Linkage Using Fully Cartesian Coordinates: A Multi-Objective Approach

María Teresa Orvañanos-Guerrero, Claudia N. Sánchez, Luis Eduardo Robles-Jiménez, Sara Carolina Gómez-Delgado

- Cartesian coordinates model six-bar mechanisms for dynamic balance optimization.
- Optimization targets shaking moment and shaking force as primary criteria.
- Multi-objective algorithms find diverse solutions faster than single-objective ones.
- Reducing counterweights from five to three retains optimal dynamic balance levels.

Highlights

Dynamic Balance Optimization of a Six-Bar Watt Linkage Using Fully Cartesian Coordinates: A Multi-Objective Approach

María Teresa Orvañanos-Guerrero, Claudia N. Sánchez, Luis Eduardo Robles-Jiménez, Sara Carolina Gómez-Delgado

- Cartesian coordinates model six-bar mechanisms for dynamic balance optimization.
- Optimization targets shaking moment and shaking force as primary criteria.
- Multi-objective algorithms find diverse solutions faster than single-objective ones.
- Reducing counterweights from five to three retains optimal dynamic balance levels.

Dynamic Balance Optimization of a Six-Bar Watt Linkage Using Fully Cartesian Coordinates: A Multi-Objective Approach

María Teresa Orvañanos-Guerrero^a, Claudia N. Sánchez^{a,b,*}, Luis Eduardo Robles-Jiménez^a and Sara Carolina Gómez-Delgado^a

^aFacultad de Ingeniería, Universidad Panamericana, Aguascalientes, 20296, Ags., Mexico

^bDepartamento de Estadística, Universidad Autónoma de Aguascalientes, Aguascalientes, 20100, Ags., México

ARTICLE INFO

Keywords:

Dynamic balancing
Six-bar Watt linkage
Multi-objective optimization
Fully Cartesian coordinates

ABSTRACT

Balancing mechanisms requires minimizing both the Shaking Moment and Shaking Force, a complex multi-criteria challenge often tackled using single-objective algorithms. However, these methods face difficulties in navigating competing objectives. In contrast, multi-objective algorithms provide a more efficient and adaptable framework, while Fully Cartesian Coordinates simplifies the balancing equations compared to conventional Cartesian formulations. This study focuses on optimizing the dynamic balance of a six-bar Watt linkage using Fully Cartesian Coordinates, comparing the performance of single-objective optimization methods—such as GA, PS, ES, DE, SRES, and ISRES—with multi-objective algorithms, including NSGA-II, NSGA-III, R-NSGA-II, R-NSGA-III, UNSGA-III, MOEA/D, AGE-MOEA, CTAEA, SMS-EMOA, and RVEA. SMS-EMOA demonstrates superior performance, achieving the highest hypervolume metric within 10.44 minutes of execution. The results indicate that multi-objective algorithms outperform single-objective approaches, offering faster and more diverse optimization solutions. Additionally, this study introduces an analytical method that enables the straightforward identification of removable counterweights, achieving an equally effective balance while minimizing the number of counterweights required.

1. Introduction

Balancing mechanisms have been a significant research focus in mechanical engineering, as effective balancing reduces vibrations, noise, and wear, enhancing both mechanical systems' performance and lifespan. The primary objective is to minimize — or ideally eliminate — the reaction forces and moments acting on the mechanism's base (shaking force and shaking moment), improving dynamic performance and operational stability while reducing maintenance costs. Various techniques have been developed to achieve optimal balance, including mass redistribution and the strategic use of counterweights [1]. Arakelian and Smith [2] explore the application of optimization algorithms and computational methods for achieving the dynamic balancing of mechanisms. They emphasize that optimization techniques enable precise mass distribution and fine-tun geometric parameters, leading to optimal balance, enhanced performance, and reduced vibrations.

This document reviews recent advancements in multi-objective optimization algorithms for balancing mechanisms, categorizing them based on the type of algorithm employed, with particular emphasis on whether they are inherently multi-objective or rely on a weighted combination of objectives. Furthermore, it examines the mathematical processes involved in deriving balancing equations. Most optimization studies have implemented these algorithms using Cartesian coordinates incorporating angular parameters. However, as demonstrated by Orvañanos et al. [33], it is possible to formulate these equations using fully Cartesian coordinates—eliminating angles and associated trigonometric functions—resulting in more computationally efficient optimization processes.

Porter *et al.* [35] presented in 1973 one of the earliest studies on dynamic balance optimization. They investigated a four-bar mechanism, formulating the objective function as a weighted sum of shaking forces, shaking moments, and joint loads. Similarly, Sadler and Mayne [29] analyzed a four-bar mechanism with counterweights, modeling the counterweights as point masses with no predefined upper limits. Their approach involved optimizing a single performance criterion while enforcing constraints on another. In 1976, Dresig *et al.* [18, 19] developed a computer-based system called KOGEOP to optimize linkage dynamics. Their research focused on minimizing an objective

 cnsanchez@up.edu.mx (C.N. Sánchez)

ORCID(s): 0000-0002-1060-0443 (M.T. Orvañanos-Guerrero); 0000-0001-6316-5214 (C.N. Sánchez)

function's mean square and peak values that integrated shaking forces, shaking moments, and driving torque. Additionally, they explored the performance of various search algorithms in the optimization process.

Walker *et al.* [47] applied optimization techniques using a nonlinear programming approach combined with the Simplex algorithm. They developed the MEDIC program, which iteratively adjusted counterweight parameters to achieve optimal balance. Their methodology employed an objective function that assigned weights to multiple criteria. Similarly, in 2013, Shankar *et al.* [44] utilized the Simplex method to optimize the shaking force of a planar four-bar mechanism, further demonstrating the effectiveness of this approach in dynamic balancing. Rao *et al.* [38] applied multi-objective optimization techniques, including goal programming, goal attainment, the lexicographic method, and the bounded objective function method, to balance a four-bar linkage mechanism. These approaches aimed to simultaneously minimize shaking forces and moments by employing weighted sum methods to construct the objective function. Qi *et al.* [37] introduced a numerically efficient technique for optimizing the dynamic balance of linkages. Their method integrates Newton's equations with the virtual work principle to decouple the link equilibrium equations, facilitating an efficient dynamic analysis. Optimization is achieved through a weighted sum approach to construct the objective function.

Multi-objective optimization techniques, which utilize methods not inherently designed for multi-objective problems in combination with mathematical approaches like weighted factors, are widely employed to explore a range of potential solutions and identify the optimal configuration that simultaneously minimizes both the shaking force and shaking moment. These techniques are particularly advantageous due to their ability to address the complex, nonlinear nature of the balancing problem, offering a set of Pareto-optimal solutions where the most suitable one can be selected based on specific performance criteria. Such advanced optimization methods have been shown to significantly enhance the dynamic performance of mechanisms, leading to improved stability and extended operational lifespan. Recent studies have introduced various approaches for optimizing the balancing of planar mechanisms using these methods. Key contributions in this field include [7], [20], [8], [9], [11], [10], [6], [12], [23], [7], [20], [8], [9], [11], [10], [12], [6], and [3]. All these optimization approaches employed traditional Cartesian coordinates methods to formulate the objective function.

Orvananos-Guerrero *et al.* [32], [33] introduced a methodology for optimizing the balance of a four-bar mechanism by formulating the objective functions exclusively in fully Cartesian coordinates. Subsequently, they extended this approach to optimize a six-bar Watt linkage [31], employing a similar technique that relied on fully Cartesian coordinates. Both studies used weighted factors to integrate the shaking forces and moments into the optimization process, enabling a balanced consideration of these dynamic parameters through a weighted combination.

Optimizing the balance of shaking force and shaking moment through multi-objective optimization algorithms can handle the problem as a set of objectives that must be minimized simultaneously. This approach eliminates the need to weigh the objectives and offers a more comprehensive solution to the balancing challenge. Notable examples of such research include the application of the Non-Dominated Sorting Genetic Algorithm II (NSGA-II [16]), an enhanced version of the original NSGA [45], and the Multi-Objective Genetic Algorithm (MOGA) to optimize the force and moment balance of a four-bar linkage, as demonstrated by Farmani *et al.* [22]. In subsequent studies, it was further employed Multi-Objective Particle Swarm Optimization (MOPSO [24], [28]) and NSGA-II to achieve similar objectives [21]. Additionally, Mejia-Rodriguez *et al.* [30] proposed a method utilizing the NSGA-II algorithm to perform robust balancing of shaking force, shaking moment, and torque in robotic manipulators.

While numerous studies have demonstrated the efficacy of various optimization algorithms in mechanism balancing, comparative analyses remain relatively scarce. This paper seeks to address this gap by conducting a comprehensive evaluation of diverse multi-objective optimization algorithms, including NSGA-II, NSGA-III, R-NSGA-II, R-NSGA-III, UNSGA-III, MOEA/D, AGE-MOEA, C-TAEA, SMS-EMOA, and RVEA. Specifically, the study minimizes the shaking force and moment in a six-bar Watt linkage. The governing equations for the optimization are derived using a mathematical method based on fully Cartesian coordinates, ensuring a straightforward yet robust and precise formulation of the dynamic problem. In addition, this document proposes a methodology to analyze the sensitivity of counterweights to determine if it is possible to reduce them.

The rest of the manuscript is organized as follows. Section 2 describes the mechanical analysis and how the mathematical equations are calculated. The optimization foundations and algorithms are introduced in Section 3. Section 4 shows the experiments and results, including the comparison of algorithms and the sensitivity analysis. Section 5 describes the balancing optimization results. And finally, Section 6 concludes this document.

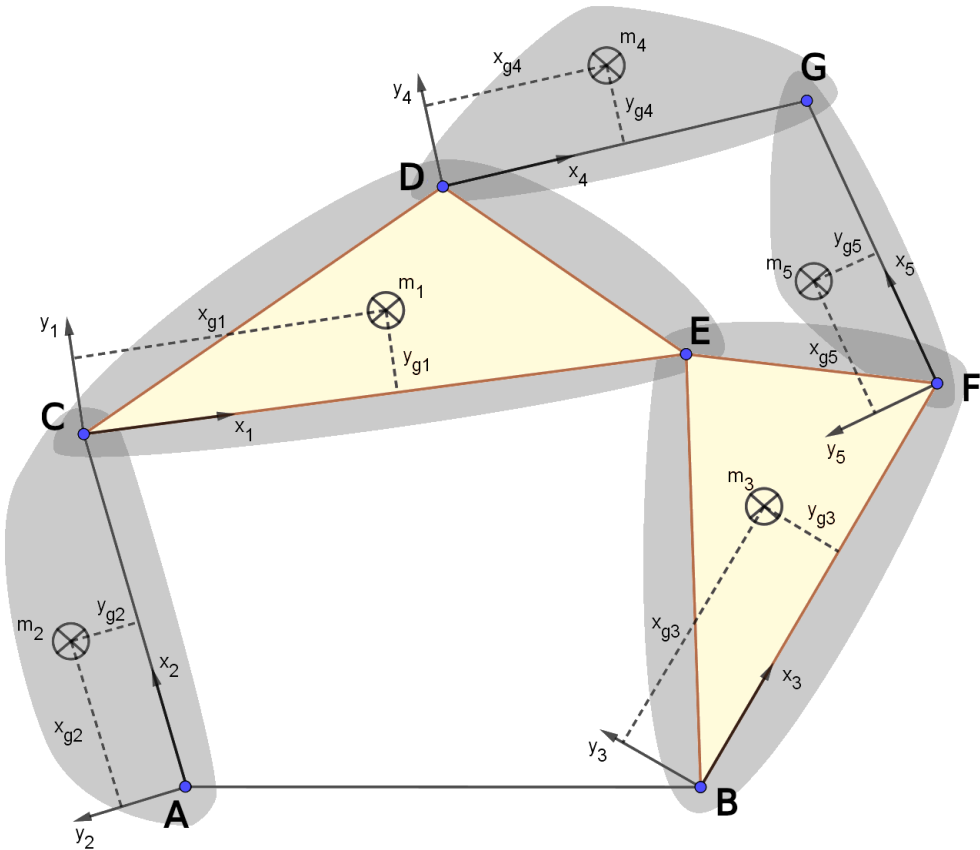


Figure 1: Six-bar Watt linkage to be optimized.

2. Mechanical Analysis

Most existing methods for optimizing mechanism balancing rely on Cartesian coordinates, which inherently involve angles and trigonometric functions for characterizing the mechanisms and formulating the corresponding balancing equations.

This section outlines the methodology for deriving the mass matrix that characterizes a six-bar Watt linkage using Fully Cartesian Coordinates (FCC), a formulation previously introduced in [31].

2.1. Mass-Matrix Characterization of a Six-Bar Watt Linkage Using FCC

Figure 1 depicts a six-bar Watt linkage consisting of five moving links and one degree of freedom. Each link is associated with a local coordinate system, where the origin is positioned at point i , and the x -axis is oriented toward point j . The physical properties of each link include its mass m_{bn} and a center of gravity defined by the local coordinates (x_{bn}, y_{bn}) for $1 \leq n \leq 5$.

Three important vectors must be defined to characterize the mass matrix of the mechanism: the vector \mathbf{q} (Eq. 1), which represents the position of the basic points; the vector $\dot{\mathbf{q}}$ (Eq. 2), which represents the velocity of the basic points; and the vector $\ddot{\mathbf{q}}$ (Eq. 3), which represents the acceleration of the basic points.

$$\mathbf{q} = [A_x \ A_y \ B_x \ B_y \ C_x \ C_y \ D_x \ D_y \ E_x \ E_y \ F_x \ F_y \ G_x \ G_y]^T \quad (1)$$

$$\dot{\mathbf{q}} = [V_{Ax} \ V_{Ay} \ V_{Bx} \ V_{By} \ V_{Cx} \ V_{Cy} \ V_{Dx} \ V_{Dy} \ V_{Ex} \ V_{Ey} \ V_{Fx} \ V_{Fy} \ V_{Gx} \ V_{Gy}]^T \quad (2)$$

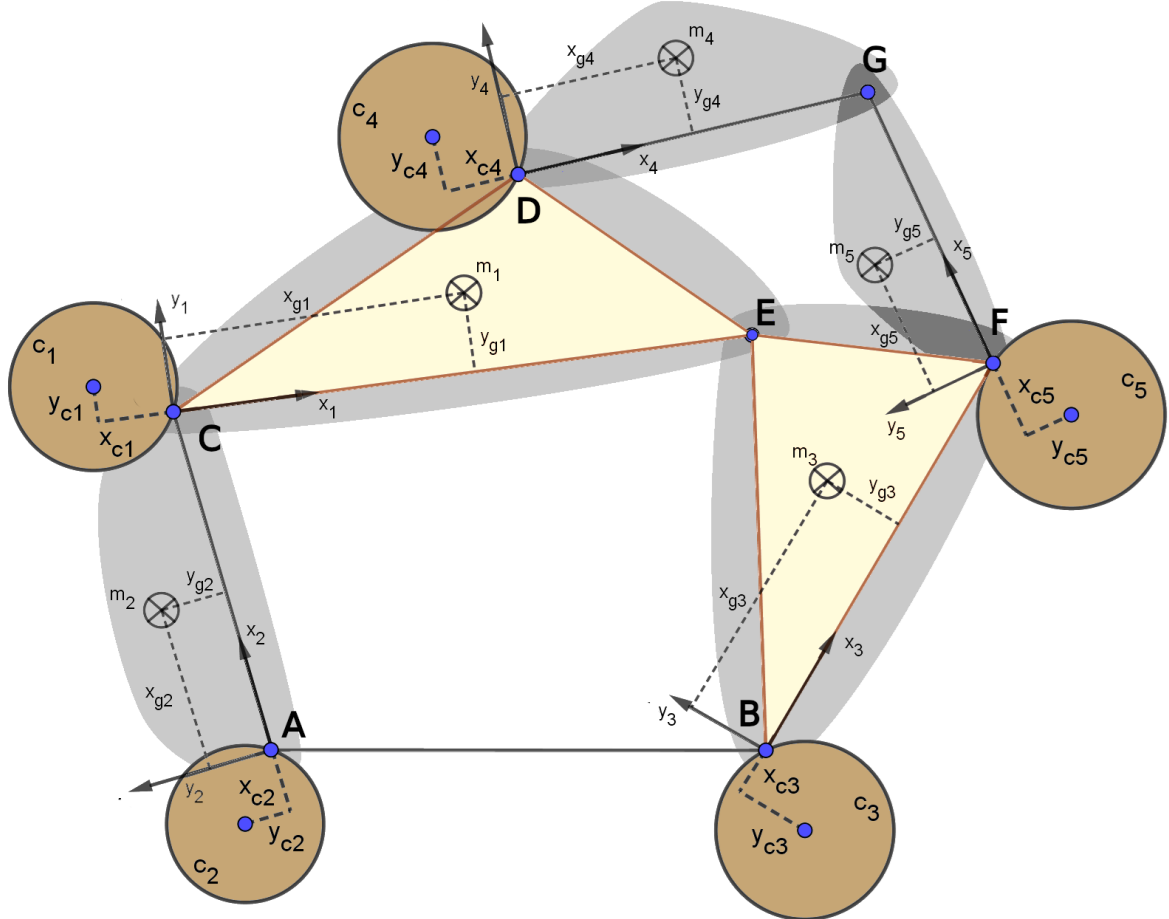


Figure 2: Six-bar Watt linkage with counterweights.

$$\ddot{\mathbf{q}} = [A_{Ax} \ A_{Ay} \ A_{Bx} \ A_{By} \ A_{Cx} \ A_{Cy} \ A_{Dx} \ A_{Dy} \ A_{Ex} \ A_{Ey} \ A_{Fx} \ A_{Fy} \ A_{Gx} \ A_{Gy}]^T \quad (3)$$

The mechanical method proposed to optimize dynamic balance in this research consists of adding fixed counterweights to each of the bars to redistribute the mass, thereby shifting the center of mass of the linkage to improve balancing. Figure 2 illustrates the mechanism with the added counterweights for each linkage. The physical properties of each counterweight include its mass m_{cn} and a center of gravity located at the local coordinates of its corresponding link, (x_{cn}, y_{cn}) , for $1 \leq n \leq 5$.

After defining the mass matrix [31] for each linkage (considering the bar-counterweight system), it is possible to derive the mass matrix that characterizes the entire mechanism.

Equation 4 presents the mass matrix M of the mechanism depicted in Figure 2, where a_n, b_n, \dots, j_n represent the elements of the individual mass matrices for each linkage, with $n = 1, \dots, 5$.

$$M = \begin{bmatrix} a_2 & 0 & 0 & 0 & b_2 & c_2 & 0 & 0 & 0 & 0 & 0 & 0 & 0 & 0 \\ 0 & a_2 & 0 & 0 & -c_2 & b_2 & 0 & 0 & 0 & 0 & 0 & 0 & 0 & 0 \\ 0 & 0 & e_3 & 0 & 0 & 0 & 0 & 0 & g_3 & 0 & f_3 & 0 & 0 & 0 \\ 0 & 0 & 0 & e_3 & 0 & 0 & 0 & 0 & 0 & g_3 & 0 & f_3 & 0 & 0 \\ b_2 & c_2 & 0 & 0 & d_2 + e_1 & 0 & g_1 & 0 & f_1 & 0 & 0 & 0 & 0 & 0 \\ -c_2 & b_2 & 0 & 0 & 0 & d_2 + e_1 & 0 & g_1 & 0 & f_1 & 0 & 0 & 0 & 0 \\ 0 & 0 & 0 & 0 & g_1 & 0 & a_4 + j_1 & 0 & i_1 & 0 & 0 & 0 & b_4 & c_4 \\ 0 & 0 & 0 & 0 & 0 & g_1 & 0 & a_4 + j_1 & 0 & i_1 & 0 & 0 & -c_4 & b_4 \\ 0 & 0 & g_3 & 0 & f_1 & 0 & i_1 & 0 & h_1 + i_3 & 0 & i_3 & 0 & 0 & 0 \\ 0 & 0 & 0 & g_3 & 0 & f_1 & 0 & i_1 & 0 & h_1 + i_3 & 0 & i_3 & 0 & 0 \\ 0 & 0 & f_3 & 0 & 0 & 0 & 0 & i_3 & 0 & a_5 + h_3 & 0 & b_5 & c_5 \\ 0 & 0 & 0 & f_3 & 0 & 0 & 0 & 0 & i_3 & 0 & a_5 + h_3 & -c_5 & b_5 \\ 0 & 0 & 0 & 0 & 0 & b_4 & c_4 & 0 & 0 & b_5 & c_5 & d_4 + d_5 & 0 \\ 0 & 0 & 0 & 0 & 0 & 0 & -c_4 & b_4 & 0 & 0 & -c_5 & b_5 & 0 & d_4 + d_5 \end{bmatrix} \quad (4)$$

The definitions of a_n , b_n , c_n , d_n , e_n , f_n , g_n , h_n , i_n , and j_n are provided in Appendix ??, where the suffix n denotes the corresponding linkage number.

2.2. Shaking Force and Shaking Moment

The mass matrix M (Eq. 4) is notable for being constant, as it is not expressed in terms of the mechanism's movement. Due to this property, it is possible to derive the equations that define the linear momentum L in both the x -axis and y -axis using Equation 5.

$$\begin{bmatrix} L_i \\ L_j \end{bmatrix} = \mathbf{B}M\dot{\mathbf{q}} \quad (5)$$

where \mathbf{B} is a matrix composed of identity matrices corresponding to the number of basic points in the mechanism (Eq. 6).

$$\mathbf{B} = \begin{bmatrix} 1 & 0 & 1 & 0 & 1 & 0 & 1 & 0 & 1 & 0 & 1 & 0 & 1 & 0 \\ 0 & 1 & 0 & 1 & 0 & 1 & 0 & 1 & 0 & 1 & 0 & 1 & 0 & 1 \end{bmatrix}^T \quad (6)$$

The Shaking Force (ShF_i and ShF_j) (Eq. 7) can be computed by taking the time derivative of the equations L_i and L_j (Eq. 5).

$$\begin{bmatrix} ShF_i \\ ShF_j \end{bmatrix} = \frac{\mathbf{B}M\ddot{\mathbf{q}}}{dt} = \mathbf{B}M\ddot{\mathbf{q}} \quad (7)$$

Similarly, the Shaking Moment (ShM) (Eq. 9) is derived by differentiating the angular momentum equation (H) (Eq. 8) with respect to time.

$$H = \mathbf{q} \times (\mathbf{M}\dot{\mathbf{q}}) = \mathbf{r}\mathbf{M}\dot{\mathbf{q}} \quad (8)$$

$$ShM = \frac{dH}{dt} = \mathbf{r}\mathbf{M}\ddot{\mathbf{q}} + \dot{\mathbf{r}}\mathbf{M}\dot{\mathbf{q}} \quad (9)$$

Considering:

$$\dot{\mathbf{r}} = [-A_Y \quad A_X \quad -B_Y \quad B_X \quad -C_Y \quad C_X \quad -D_Y \quad D_X \quad -E_Y \quad E_X \quad -F_Y \quad F_X \quad -G_Y \quad G_X]^T \quad (10)$$

$$\dot{\mathbf{r}} = [-VA_Y \quad VA_X \quad -VB_Y \quad VB_X \quad -VC_Y \quad VC_X \quad -VD_Y \quad VD_X \\ -VE_Y \quad VE_X \quad -VF_Y \quad VF_X \quad -VG_Y \quad VG_X]^T \quad (11)$$

3. Optimization

Numerical optimization involves identifying the optimal solution (maximum or minimum) to a mathematical problem through systematically evaluating and refining candidate solutions using numerical methods. Such problems typically comprise an objective function dependent on one or more variables, subject to constraints. In the present context, the objective functions to be optimized are the Shaking Force (ShF) and the Shaking Moment (ShM). The design variables consist of the positions and thicknesses of the counterweights.

This section formally defines the objective functions, variables, and constraints. Furthermore, it details the various single- and multi-objective optimization algorithms employed to optimize the six-bar Watt linkage.

3.1. Objective Functions and Boundaries

This study considers the Shaking Force $ShF(X)$ and the Shaking Moment $ShM(X)$ as the objective functions for optimizing the balance of the mechanism. To ensure dimensionless quantities for $ShF(X)$ and $ShM(X)$, normalization factors $\beta_{ShF}(X)$ and $\beta_{ShM}(X)$ are introduced, defined as follows:

$$\beta_{ShF}(X) = \frac{rms(^oShF(X))}{rms(ShF(X))} = \sqrt{\frac{\sum_{k=1}^N (^oShF_{ik}(X)^2 + ^oShF_{jk}(X)^2)}{\sum_{k=1}^N (ShF_{ik}(X)^2 + ShF_{jk}(X)^2)}} \quad (12)$$

$$\beta_{ShM}(X) = \frac{rms(^oShM(X))}{rms(ShM(X))} = \sqrt{\frac{\sum_{k=1}^N ^oShM_k(X)^2}{\sum_{k=1}^N ShM_k(X)^2}} \quad (13)$$

$\beta_{ShF}(X)$ (Eq. 12) is defined as the ratio of the root mean square (RMS) value of the shaking force reaction for the optimized mechanism ($rms(^oShF(X))$) to the RMS value of the shaking force for the original, unbalanced mechanism ($rms(ShF(X))$), both evaluated over a time period T . The values of \mathbf{q} , $\dot{\mathbf{q}}$, and $\ddot{\mathbf{q}}$ for each time step k can be obtained through direct kinematics or by modeling the original mechanism using CAD software, such as Solidworks.

Analogously, $\beta_{ShM}(X)$ (Eq. 13) is determined by a similar ratio, where $^oShM(X)$ represents the Shaking Moment of the optimized mechanism, and $ShM(X)$ is a constant representing the Shaking Moment of the unbalanced mechanism.

A solution to the problem, X (Eq. 14), is a vector comprising all the design variables associated with the five counterweights.

$$X = [x_1, y_1, t_1, x_2, y_2, t_2, x_3, y_3, t_3, x_4, y_4, t_4, x_5, y_5, t_5] \quad (14)$$

The constraints on the design variables, corresponding to the mass center position (x_i, y_i) and the thickness (t_i) of each counterweight ($1 \leq i \leq 5$), are imposed based on the physical limitations of the model and are defined in Eq. 15.

$$\begin{aligned} -0.16 &\leq x_i \leq 0.16 \\ -0.16 &\leq y_i \leq 0.16 \\ 0.005 &\leq t_i \leq 0.04 \end{aligned} \quad (15)$$

3.2. Single- and Multi-Objective Optimization

Numerical optimization algorithms can be broadly classified as single- or multi-objective. Single-objective optimization algorithms aim to optimize (minimize or maximize) a single objective function. As previously defined, the problem of balancing the six-bar Watt linkage involves two objective functions: $\beta_{ShM}(X)$ and $\beta_{ShF}(X)$. Prior work

[31, 33] employed a single-objective optimization approach by constructing a linear combination of the objectives, as shown in Eq. 16, where γ is a hyperparameter ranging from 0 to 1, controlling the relative weight assigned to each objective function.

$$f(X) = \gamma \beta_{ShM}(X) + (1 - \gamma) \beta_{ShF}(X) \quad (16)$$

However, this research compares the performance of single- and multi-objective algorithms.

Multi-objective optimization algorithms address problems involving two or more conflicting objectives [14], as is the case with $\beta_{ShF}(X)$ and $\beta_{ShM}(X)$. These algorithms aim to identify a set of solutions that balance these competing objectives. A single, universally "best" solution rarely exists in multi-objective optimization. Instead, a given solution may excel for one objective but perform poorly with respect to another.

To assess solution quality, solutions are categorized as either dominated or non-dominated. A solution X_d is considered dominated by another solution X_o if the following two conditions are met:

- X_o is at least as good as X_d in all objectives.

$$\beta_{ShM}(X_o) \leq \beta_{ShM}(X_d) \text{ and } \beta_{ShF}(X_o) \leq \beta_{ShF}(X_d) \quad (17)$$

- X_o is strictly better in at least one objective than X_d .

$$\beta_{ShM}(X_o) < \beta_{ShM}(X_d) \text{ or } \beta_{ShF}(X_o) < \beta_{ShF}(X_d) \quad (18)$$

A solution is considered non-dominated if no other solution exists that dominates it. Non-dominated solutions are also called Pareto-optimal solutions, representing trade-offs where improvement in one objective necessitates a degradation in the other one.

Hypervolume is a widely adopted indicator in multi-objective optimization for evaluating the quality of a solution set. The hypervolume indicator quantifies the "size of the space covered" [43]. Higher hypervolume values indicate a superior solution set, implying a larger region of dominance and typically better proximity to the Pareto-optimal front. This metric simultaneously assesses two key aspects: convergence, reflecting how close the solutions are to the Pareto-optimal front, and diversity, indicating how well the solutions are distributed across the front.

3.3. Algorithms

This research optimizes balancing a six-bar Watt linkage, comparing the performance of sixteen optimization algorithms: six single-objective and ten multi-objective.

The single-objective algorithms evaluated in this study include Differential Evolution (DE), Evolution Strategy (ES), Genetic Algorithm (GA), Improved Stochastic Ranking Evolution Strategy (ISRES), Stochastic Ranking Evolution Strategy (SRES), and Pattern Search (PS). The multi-objective optimization algorithms investigated are Non-dominated Sorting Genetic Algorithm II (NSGA-II), NSGA-III, R-NSGA-II, R-NSGA-III, UNSGA-III, Multi-objective Evolutionary Algorithm based on Decomposition (MOEA/D), Adaptive Geometric-based Multi-objective Evolutionary Algorithm (AGE-MOEA), Convergence and Trade-off-based Multi-objective Evolutionary Algorithm (C-TAEA), S-Metric Selection Evolutionary Multiobjective Optimization Algorithm (SMS-EMOA), and Reference Vector Guided Evolutionary Algorithm (RVEA).

Section 3.3.1 concisely describes each single-objective optimization algorithm employed in this research. Conversely, Section 3.3.2 details the multi-objective optimization algorithms.

3.3.1. Single-Objective Optimization Algorithms

The Genetic Algorithm (GA) was introduced by Holland, J. in the 1960s and formalized in his 1975 book [25]. Inspired by natural selection in biological evolution, it employs selection, crossover, and mutation to iteratively refine solutions.

The Pattern Search (PS) algorithm [26], introduced by Hooke, R., et al. in 1961, is a direct search method. It iteratively evaluates candidate solutions within a structured pattern, adjusting the search area based on the observed results. Pattern search is particularly well-suited for objective functions that are non-smooth, non-linear, or noisy.

The Evolution Strategy (ES) algorithm [39], developed by Rechenberg, I. in 1978, is another evolutionary algorithm that aims to evolve a population of candidate solutions to identify the optimal one. This algorithm is based on Gaussian random mutations, with optional recombination, and often employs self-adaptive step sizes for local exploration.

Differential Evolution (DE) [36], developed by Kenneth Price and published in 1994, is a biologically inspired optimization algorithm that maintains a population of candidate solutions. It generates new candidate solutions using mathematical operations based on differences between randomly selected individuals within the population and ensures the preservation of superior solutions.

In 2000, Runarsson, T.P., and Yao, X., developed the Stochastic Ranking for Constrained Evolutionary Optimization (SRES) algorithm [40]. This derivative-free global optimization method is designed for solving constrained optimization problems by combining fitness values and constraint violation information into a single ranking system.

The Improved Stochastic Ranking Evolution Strategy (ISRES) algorithm [41], proposed by Runarsson, T.P., et al. in 2005, is specifically tailored for constrained optimization and is particularly effective in addressing non-linear problems. This algorithm combines stochastic search and evolutionary strategies.

3.3.2. Multi-Objective Optimization Algorithms

The Non-dominated Sorting Genetic Algorithm II (NSGA-II), developed by Kalyanmoy et al. [16] in 2002, is characterized by non-dominated sorting, crowding distance calculation, elitism, fast computation, and genetic operations such as crossover and mutation to generate new solutions.

In 2006, Kalyanmoy et al. [17] introduced R-NSGA-II, incorporating decision-maker preferences through reference points to more effectively guide the search for desirable solutions.

Kalyanmoy and Himanshu developed NSGA-III [15] in 2013. This algorithm modifies specific selection mechanisms of NSGA-II to enhance the diversity of the resulting solutions.

The Unified NSGA-III (UNSGA-III) algorithm [42], an extension of NSGA-III developed by Seada and Kalyanmoy in 2015, aims to improve performance and broaden applicability in multi-objective optimization. It integrates several techniques and concepts for more efficient handling of multi-objective problems, including a unified approach for diversity maintenance, reference point management, and solution selection, thereby enhancing its versatility.

The Reference-point based NSGA-III (R-NSGA-III) algorithm [46], designed by Vesikar et al. in 2018, builds upon NSGA-III by incorporating user-defined reference points. This allows users to specify preferred regions within the objective space, guiding the search towards solutions of interest.

A distinct approach to multi-objective optimization was introduced by Zhang and Li in 2007 with the Multi-objective Evolutionary Algorithm based on Decomposition (MOEA/D) [48]. This method decomposes a multi-objective optimization problem into a set of scalar optimization subproblems and then solves them concurrently by integrating evolutionary algorithms with a decomposition strategy.

2019 Panichella introduced the Adaptive Geometry Estimation based MOEA (AGE-MOEA) [34], an adaptive generalized multi-objective evolutionary algorithm. While it follows the general structure of NSGA-II, it employs a modified crowding distance calculation. This algorithm incorporates an adaptive framework that adjusts parameters or strategies based on the evolving optimization process.

Also in 2019, Li et al. introduced the Convergence and Trade-off-based Multi-objective Evolutionary Algorithm (C-TAEA) [27] for solving multi-objective problems. This algorithm emphasizes both convergence to the Pareto front and the maintenance of a well-distributed set of solutions.

The S-Metric Selection Evolutionary Multiobjective Optimization Algorithm (SMS-EMOA), introduced by Beume et al. [4] in 2007, is specifically designed to maximize the dominated hypervolume during the optimization process. It employs the s-metric (referring to the hypervolume measure) as a central component in its selection process, effectively guiding the population of solutions toward a diverse and high-quality representation of the Pareto front.

The Reference Vector Guided Evolutionary Algorithm (RVEA), presented by Cheng et al. [13] in 2016, utilizes reference vectors in the objective space to guide the population toward the Pareto front while maintaining diversity. It incorporates an angle penalty function to dynamically balance convergence and diversity.

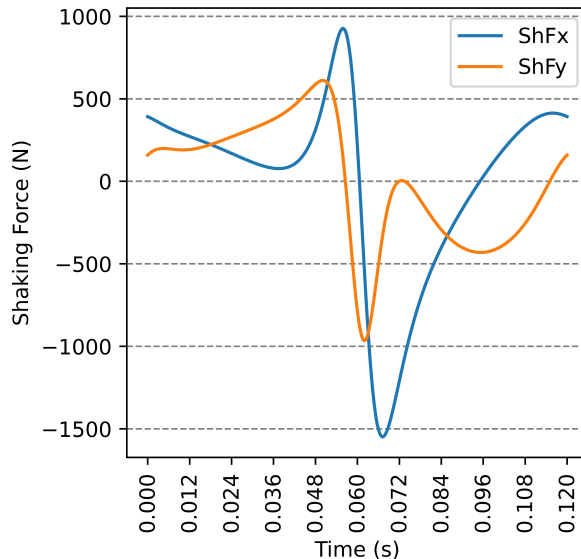
4. Experiments and Results

This section presents the experiments and results obtained from optimizing the dynamic balance of a six-bar Watt linkage modeled using Fully Cartesian Coordinates. It is organized into three subsections to facilitate the analysis and interpretation of the performance of different optimization algorithms and the sensitivity of key features.

Table 1

Parameters of the six-bar Watt linkage. Parameters indicated with a ‘–’ are unnecessary for the numerical analysis.

Link n	1	2	3	4	5
Mass m_{b_n} [kg]	0.6935	0.1022	0.9636	0.1825	0.1679
Length l_n [m]	0.19	0.14	0.1341640	0.25	0.23
Inertia I_{xb_n} [kg · m ²]	0.0011616	-	0.0062264	-	-
Inertia I_{yb_n} [kg · m ²]	0.0055653	-	0.0065733	-	-
Inertia I_{zb_n} [kg · m ²]	-	0.0006685	-	0.0038036	0.0029620
Inertia I_{xyb_n} [kg · m ²]	0.0016759	-	0.0052291	-	-
CoM x_{b_n} [m]	0.08	0.07	0.0775170	0.125	0.115
CoM y_{b_n} [m]	0.0333333	0.0	0.0655913	0.0	0.0
K_x [m]	0.05	-	0.0983869	-	-
K_y [m]	0.1	-	0.1966773	-	-

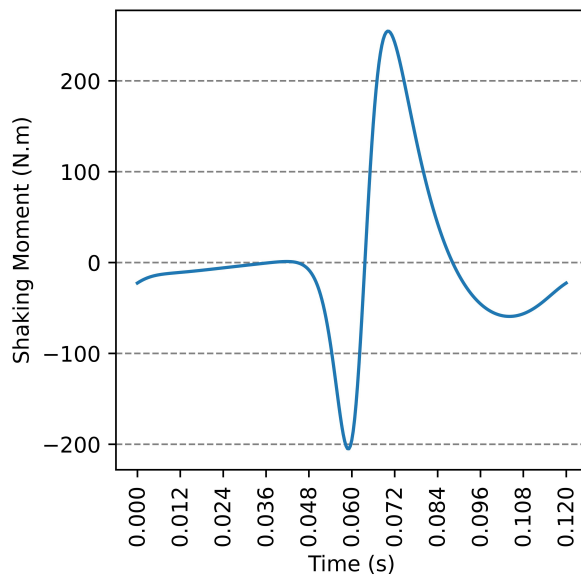
**Figure 3:** Unbalanced Shaking Force

Subsection 4.1 details the physical properties of the six-bar Watt linkage in its uncompensated state (i.e., without counterweights). Subsection 4.2 analyzes the performance of various optimization techniques, encompassing single-objective and multi-objective algorithms. Finally, Subsection 4.3 presents a sensitivity analysis of the solutions identified by the most effective algorithm.

4.1. Physical Properties of the Six-Bar Watt Linkage without Counterweights

Table 1 presents the physical properties of the six-bar Watt linkage illustrated in Figure 1. The links are assumed to be fabricated from steel with a density of $7800\text{kg}/\text{m}^3$, while the counterweights are brass, with a density of $\rho_{cn} = 8500\text{kg}/\text{m}^3$.

The behavior of the Shaking Force (along the x and y axes) and the Shaking Moment before balance optimization are illustrated in Figures 3 and 4, respectively.

**Figure 4:** Unbalance Shaking Moment

4.2. Comparison of Different Optimization Algorithms

This subsection compares the performance of various single-objective (GA, DE, ES, SRES, ISRES, PS) and multi-objective (NSGA-II, NSGA-III, R-NSGA-II, R-NSGA-III, UNSGA-III, MOEA/D, AGE-MOEA, C-TAEA, SMS-EMOA, RVEA) algorithms when applied to the dynamic balance optimization of a six-bar Watt linkage.

The optimization algorithms were implemented in Python using the Pymoo library [5]. A consistent set of hyperparameters was employed for all algorithms: a population size of 150 individuals and 500 generations. All other hyperparameters were set to their default values.

The multi-objective optimization algorithms were executed once, generating solutions that constitute the Pareto front. Conversely, each single-objective optimization algorithm was executed 200 times, each run employing a randomly selected value of γ (ranging from 0 to 1) to define the objective function, as described in Equation 16.

Figures 5 and 6, along with Table 2, present the performance of the single- and multi-objective optimization algorithms with respect to ShM and ShF, visualized through the Pareto fronts of the obtained solutions. Figure 6 shows that the multi-objective algorithms identified a larger number of solutions. Most solutions found by the single-objective algorithms lie along or near the Pareto front. Visual comparison of Figures 5 and 6 does not readily reveal a single best-performing algorithm. However, analysis of the multi-objective algorithms suggests that NSGA-III, R-NSGA-III, AGE-MOEA, and SMS-EMOA demonstrate strong performance. Table 2 presents the hypervolume metric calculated from the Pareto front solutions obtained by each algorithm. This metric identifies SMS-EMOA as the most effective algorithm for optimizing the ShM and ShF objective functions.

Table 3 presents the execution times for both single- and multi-objective optimization algorithms. A significant difference in execution times is observed between the two categories. This disparity arises because single-objective algorithms require multiple executions to generate a set of solutions approximating the Pareto front. Multi-objective algorithms, conversely, can generate a diverse set of solutions within a single execution. Among the tested algorithms, C-TAEA and MOEA/D exhibited the shortest execution times; however, as illustrated in Figure 6, their performance in terms of solution quality was not optimal. In contrast, SMS-EMOA, which demonstrated the best performance with respect to ShM and ShF (see Table 2), had an execution time of 10.44 minutes—considerably faster than the single-objective algorithms, which required over 500 minutes to complete their multiple runs.

4.3. Analysis of Solutions Obtained with the Best Algorithm

The previous experiment identified SMS-EMOA as the best-performing multi-objective optimization algorithm, achieving the highest hypervolume with an execution time of 10.44 minutes. The solutions generated by this algorithm (shown in Figure 6) were subsequently used for sensitivity analysis.

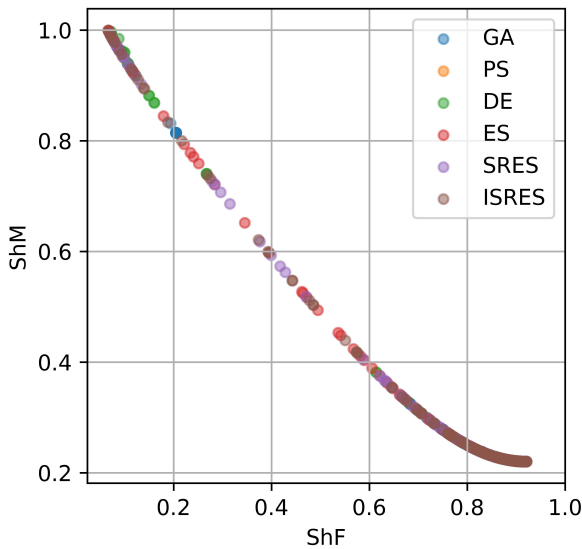


Figure 5: Performance of single-objective optimization algorithms in terms of ShM and ShF

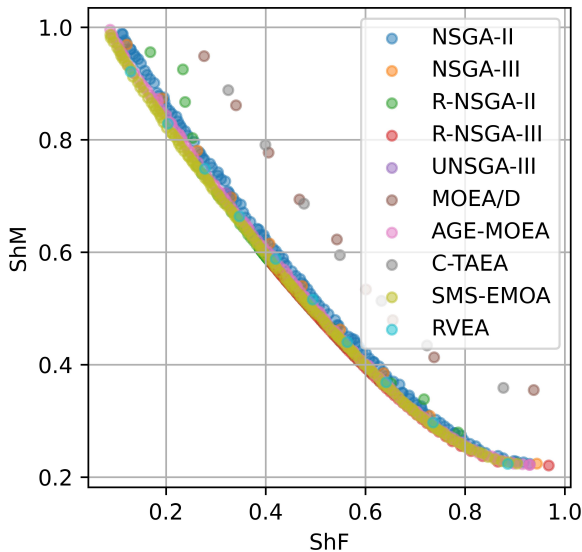


Figure 6: Performance of multi-objective optimization algorithms in terms of ShM and ShF

Figure 7 displays boxplots of the feature values corresponding to the best solutions identified by SMS-EMOA. It is observed that the x and y values for counterweights 4 and 5 are near zero. Furthermore, the thicknesses of these counterweights are very small, approaching the minimum bound (see Equation 15); the average thicknesses are 0.0068 and 0.0059 for counterweights 4 and 5, respectively. This suggests that these counterweights contribute minimally to optimizing the ShM and ShF objective functions. Some features exhibit more significant variance than others; for instance, y_{3c} assumes both negative and positive values.

Figure 8 presents the feature values, categorized according to the corresponding ShM and ShF values. It is observed that the values of y_{3c} play a critical role in determining whether the mechanism tends to optimize ShM or ShF: negative values correspond to ShM optimization, while positive values favor ShF optimization. A similar pattern is evident for

Table 2

Hypervolume of different optimization algorithms

Algorithm	Type	Hypervolume
GA	Single	0.327
PS	Single	0.24
DE	Single	0.39
ES	Single	0.452
SRES	Single	0.441
ISRES	Single	0.448
NSGA-II	Multi	0.438
NSGA-III	Multi	0.405
R-NSGA-II	Multi	0.427
R-NSGA-III	Multi	0.387
UNSGA-III	Multi	0.201
MOEA/D	Multi	0.297
AGE-MOEA	Multi	0.454
C-TAEA	Multi	0.291
SMS-EMOA	Multi	0.458
RVEA	Multi	0.422

Table 3

Execution time of different multi-objective optimization algorithms

Algorithm	Time per repetition (min)	No. Repetitions	Total time (min)
GA	13.43	200	2686.0
PS	2.66	200	532.0
DE	13.3	200	2660.0
ES	26.62	200	5324.0
SRES	26.62	200	5324.0
ISRES	26.48	200	5296.0
NSGA-II	13.15	1	13.15
NSGA-III	10.86	1	10.86
R-NSGA-II	10.23	1	10.23
R-NSGA-III	21.09	1	21.09
UNSGA-III	10.32	1	10.32
MOEA/D	0.96	1	0.96
AGE-MOEA	10.56	1	10.56
C-TAEA	0.87	1	0.87
SMS-EMOA	10.44	1	10.44
RVEA	10.43	1	10.43

y_{1c} . A trend is also observed for t_{2c} : lower thickness values tend to correlate with ShF optimization, whereas higher thickness values are more effective for ShM optimization.

As shown in Figure 7, counterweights four and five tend to be minimized or effectively eliminated. Therefore, the SMS-EMOA algorithm was re-executed with modified parameters. First, counterweights four and five were removed while maintaining the original constraints. Subsequently, a second experiment was conducted in which counterweights four and five were removed, and the thickness constraint was increased, allowing a maximum value of 0.10. This adjustment was implemented because the thickness values of counterweights one, two, and three are close to the maximum allowable value (see Figures 7 and 8).

Figure 9 presents the results of these experiments. It can be observed that using only the first three counterweights, or including all five, yields comparable results in terms of ShM and ShF optimization. This finding is significant, suggesting that two counterweights can be eliminated without compromising the optimization performance. Furthermore,

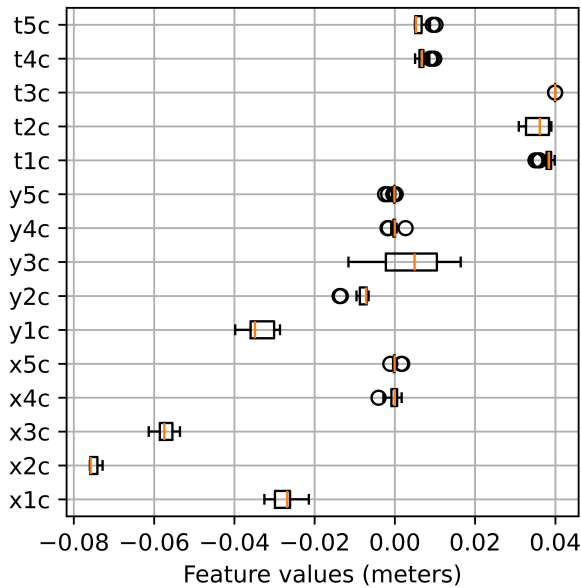


Figure 7: Boxplots of features values for the best solutions obtained with SMS-EMOA

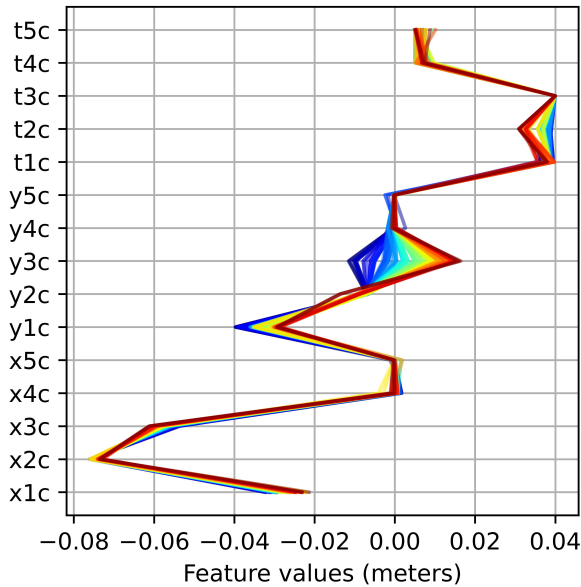


Figure 8: Feature Values of the Best Solutions Obtained with SMS-EMOA, Based on ShM and ShF. Each line represents a solution. The bluer the line, the lower the value of ShF, while the redder the line, the higher the value of ShF. Conversely, the bluer the line, the higher the value of ShM, and the redder the line, the lower the value of ShM.

increasing the maximum allowable thickness t_n to 0.10 m enables smaller ShM and ShF values to be achieved. While a thickness of 0.10 m may not be practical for the current mechanism design, this observation provides valuable insight for future work, suggesting exploring alternative designs or materials.

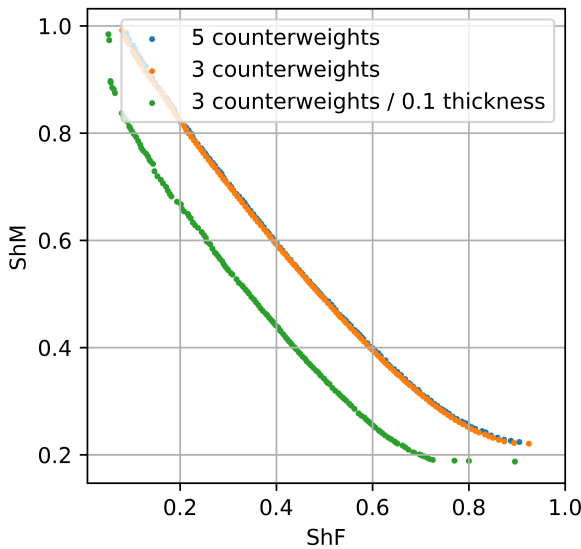


Figure 9: Comparison of using five or three counterweights and incrementing the thickness constraint.

5. Balancing Optimization Results

The optimal solution for balancing a six-bar Watt linkage is application-dependent. Solutions can be selected from the Pareto front, enabling a choice that prioritizes either ShF or ShM minimization or achieves a balanced reduction in both.

For example, consider the solution obtained by SMS-EMOA (Eq. 19), corresponding to $\beta_{ShF}(X) = 0.088122439$ and $\beta_{ShM}(X) = 0.986658705$. This solution yields a 91.19% reduction in ShF, while ShM is only reduced by 1.33%.

$$\begin{aligned} X = [& -0.030831847, -0.039661495, 0.035057972, -0.07599735, \\ & -0.007025791, 0.038659613, -0.053661036, -0.011334326, \\ & 0.039975214, 0.001697872, -0.000244507, 0.006851988, \\ & 3.28 \times 10^{-6}, -0.000192983, 0.005291985] \end{aligned} \quad (19)$$

Figures 10 and 11 compare the unbalanced and balanced Shaking Force (both ShF_x and ShF_y) and the unbalanced and balanced Shaking Moment (ShM) using the solution vector provided in Equation 19.

Alternatively, consider the solution obtained by SMS-EMOA (Eq. 20), corresponding to $\beta_{ShM}(X) = 0.223958809$ and $\beta_{ShF}(X) = 0.904631455$. This solution yields a 77.60% reduction in ShM, while ShF is reduced by 9.54%.

$$\begin{aligned} X = [& -0.021412978, -0.029195457, 0.037784463, -0.073448194, \\ & -0.013638246, 0.030923509, -0.061095557, 0.016437665, \\ & 0.039998554, -4.81 \times 10^{-5}, -0.000899927, 0.007440477, \\ & -6.51 \times 10^{-5}, -0.000255341, 0.005009233] \end{aligned} \quad (20)$$

Figures 12 and 13 illustrate a comparison between the unbalanced and balanced Shaking Force (both ShF_x and ShF_y) and the unbalanced and balanced Shaking Moment (ShM) using the solution vector presented in Equation 20.

Finally, consider the solution obtained by SMS-EMOA (Eq. 21), corresponding to $\beta_{ShF}(X) = 0.495728512$ and $\beta_{ShM}(X) = 0.495578094$. This solution yields a 50.43% reduction in ShF and a 50.44% reduction in ShM.

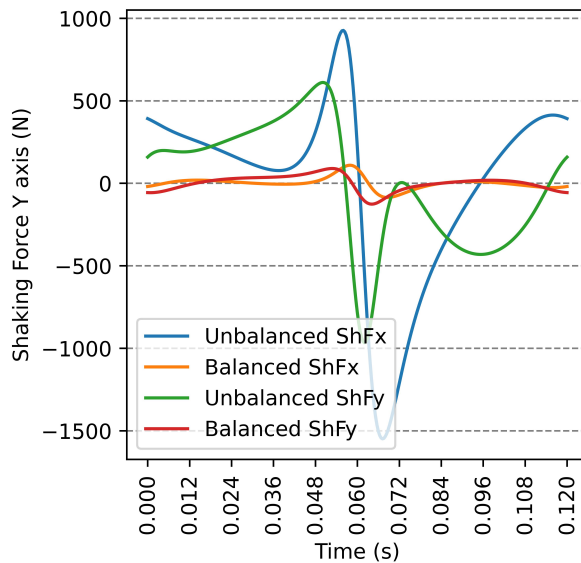


Figure 10: Comparison between unbalanced and balanced Shaking Force for the solution vector presented in Eq. 19

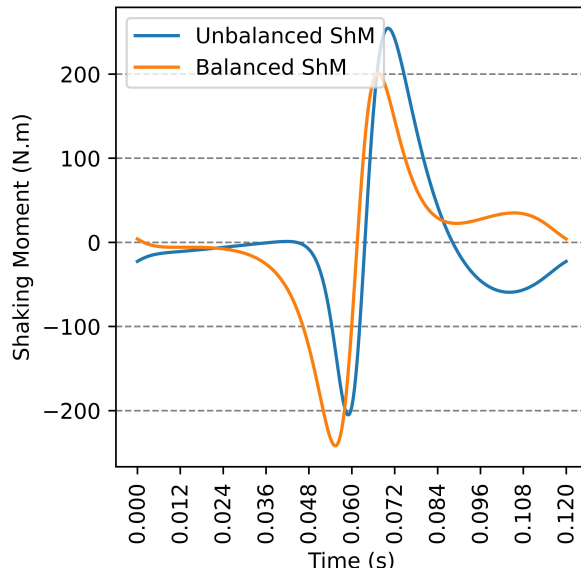


Figure 11: Comparison between unbalanced and balanced Shaking Moment for the solution vector presented in Eq. 19

$$X = [-0.026785451, -0.033672311, 0.038997486, -0.074123172, \\ -0.006617802, 0.037072145, -0.057625145, 0.006778145, \\ 0.039998738, -0.000835092, -2.45 \times 10^{-5}, 0.005474983, \\ -0.000293343, 0.000177994, 0.005078357] \quad (21)$$

Figure 15 presents a comparison between the unbalanced and balanced Shaking Force (both ShF_x and ShF_y) and the unbalanced and balanced Shaking Moment (ShM) using the solution vector provided in Equation 21.

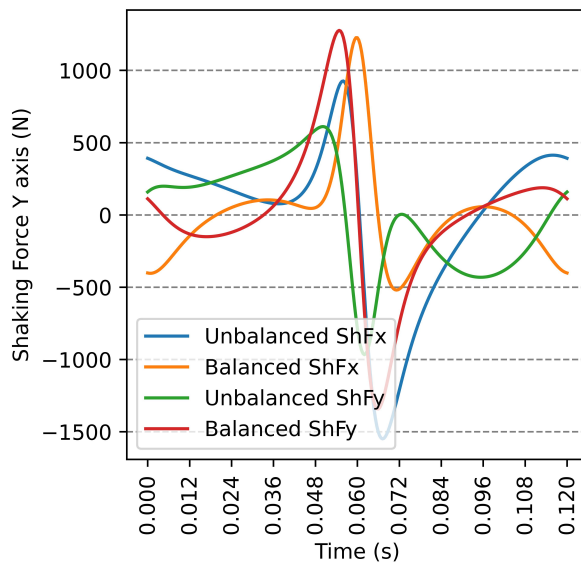


Figure 12: Comparison between unbalanced and balanced Shaking Force for the solution vector presented in Eq. 20

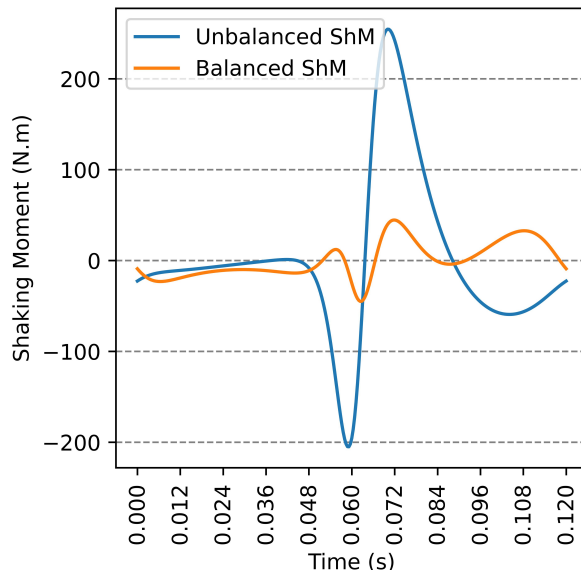


Figure 13: Comparison between unbalanced and balanced Shaking Moment for the solution vector presented in Eq. 20

6. Conclusion

This paper presented the dynamic balance optimization of a six-bar Watt linkage modeled using Fully Cartesian coordinates (also known as Natural coordinates), comparing the performance of single- and multi-objective optimization algorithms. While much of the current state-of-the-art mechanism balancing optimization relies on Cartesian coordinates and single-objective algorithms, the balancing problem involves two quantities: Shaking Moment and Shaking Force. Using multi-objective algorithms offers a more efficient approach to balancing optimization, enabling identifying a wider range of solutions in a shorter timeframe.

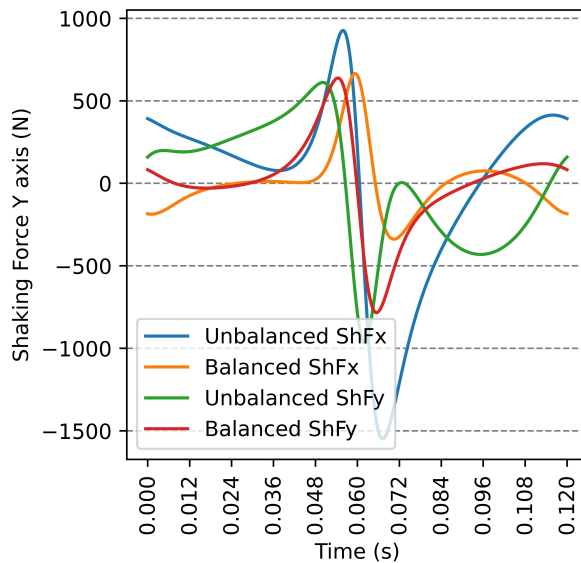


Figure 14: Comparison between unbalanced and balanced Shaking Force for the solution vector presented in Eq. 21

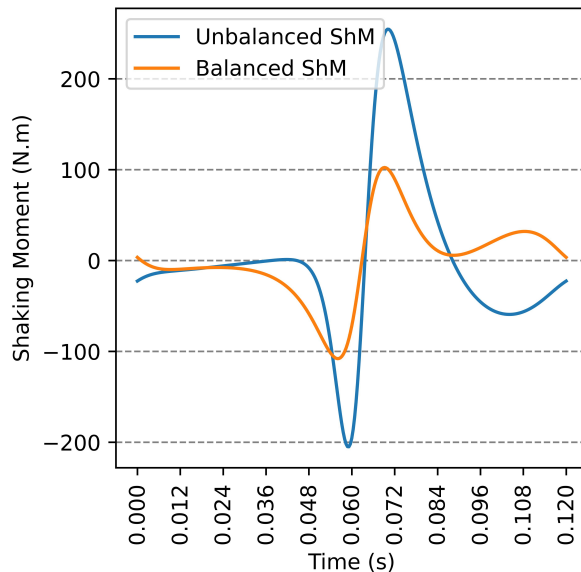


Figure 15: Comparison between unbalanced and balanced Shaking Moment for the solution vector presented in Eq. 21

This research compared the performance of single-objective (GA, ES, DE, SRES, and ISRES) and multi-objective (NSGA-II, NSGA-III, R-NSGA-II, R-NSGA-III, UNSGA-III, MOEA/D, AGE-MOEA, C-TAEA, SMS-EMOA, and RVEA) algorithms. SMS-EMOA emerged as the top performer, exhibiting the highest hypervolume and an execution time of 10.44 minutes. The experiments demonstrated that multi-objective algorithms are significantly more efficient at identifying diverse solutions than single-objective algorithms, establishing them as the preferred method for balancing mechanical systems.

Sensitivity analysis revealed that two counterweights could be eliminated without affecting the optimization performance achieved with all five counterweights. Further analysis identified the y -position of the third counterweight

and the thickness t of the second counterweight as critical parameters influencing whether the optimization prioritizes Shaking Moment or Shaking Force reduction.

The analysis presented in this research demonstrates that the SMS-EMOA optimization algorithm can achieve either a 91.19% reduction in Shaking Force (with a corresponding 1.33% reduction in Shaking Moment) or a 77.60% reduction in Shaking Moment (with a corresponding 9.54% reduction in Shaking Force).

Acknowledgments

The authors gratefully acknowledge the financial support provided by the Instituto de Ciencia y Tecnología del Estado de Aguascalientes (INCYTEA) for equipment procurement through the project "Análisis y optimización del balanceo de mecanismos utilizando coordenadas naturales." María T. Orvañanos-Guerrero extends her sincere appreciation to INCYTEA for their generous support.

References

- [1] Arakelian, V., Dahan, M., Smith, M., 2000. A Historical Review of the Evolution of the Theory on Balancing of Mechanisms, in: International Symposium on History of Machines and Mechanisms Proceedings HMM 2000. Springer Netherlands, Dordrecht, pp. 291–300. doi:10.1007/978-94-015-9554-4.
- [2] Arakelian, V.H., Smith, M.R., 2005. Shaking force and shaking moment balancing of mechanisms: A historical review with new examples. *Journal of Mechanical Design* 127, 334–339. doi:10.1115/1.1829067.
- [3] Belleri, B.K., Kerur, S.B., 2021. Balancing of planar six-bar mechanism with genetic algorithm. *Journal of Mechanical and Energy Engineering* 4, 303–308. doi:10.30464/jmee.2020.4.4.303.
- [4] Beume, N., Naujoks, B., Emmerich, M., 2007. SMS-EMOA: Multiobjective selection based on dominated hypervolume. *European Journal of Operational Research* 181, 1653–1669. doi:10.1016/j.ejor.2006.08.008.
- [5] Blank, J., Deb, K., 2020. pymoo: Multi-objective optimization in python. *IEEE Access* 8, 89497–89509. doi:10.1109/ACCESS.2020.2990567.
- [6] Chaudhary, H., Chaudhary, K., 2016a. Design of reactionless mechanisms based on constrained optimization procedure. *Dynamic Balancing of Mechanisms and Synthesizing of Parallel Robots*, 273–298doi:10.1007/978-3-319-17683-3.
- [7] Chaudhary, H., Saha, S.K., 2008. Balancing of shaking forces and shaking moments for planar mechanisms using the equimomental systems. *Mechanism and Machine Theory* 43, 310–334. doi:10.1016/j.mechmachtheory.2007.04.003.
- [8] Chaudhary, K., Chaudhary, H., 2013. Minimization of Shaking Force and Shaking Moment in Multiloop Planar Mechanisms, in: 1st International and 16th National Conference on Machines and Mechanisms.
- [9] Chaudhary, K., Chaudhary, H., 2014. Dynamic balancing of planar mechanisms using genetic algorithm. *Journal of Mechanical Science and Technology* 28, 4213–4220. doi:10.1007/s12206-014-0934-4.
- [10] Chaudhary, K., Chaudhary, H., 2015a. Optimum Dynamic Balancing of a Planar Five-Bar Mechanisms Using Genetic Algorithm, in: International Conference on Advances in Materials and Product Design, AMPD, Gujarat, India.
- [11] Chaudhary, K., Chaudhary, H., 2015b. Shape Optimization of Dynamically Balanced Planar Four-bar Mechanism, in: Procedia Computer Science, Elsevier, pp. 519–526. doi:10.1016/j.procs.2015.07.378.
- [12] Chaudhary, K., Chaudhary, H., 2016b. Optimal dynamic design of planar mechanisms using teaching-learning-based optimization algorithm. *Proceedings of the Institution of Mechanical Engineers, Part C: Journal of Mechanical Engineering Science* 230, 3442–3456. doi:10.1177/0954406215612831.
- [13] Cheng, R., Jin, Y., Olhofer, M., Sendhoff, B., 2016. A Reference Vector Guided Evolutionary Algorithm for Many-Objective Optimization. *IEEE Transactions on Evolutionary Computation* 20, 773–791. doi:10.1109/TEVC.2016.2519378.
- [14] Collette, Y., Siarry, P., 2004. Multiobjective Optimization doi:10.1007/978-3-662-08883-8.
- [15] Deb, K., Jain, H., 2013. An evolutionary many-objective optimization algorithm using reference-point-based nondominated sorting approach, part i: solving problems with box constraints. *IEEE Transactions on Evolutionary Computation* 18, 577–601. doi:10.1109/TEVC.2013.2281535.
- [16] Deb, K., Pratap, A., Agarwal, S., Meyarivan, T., 2002. A Fast and Elitist Multiobjective Genetic Algorithm: NSGA-II, in: *IEEE Transactions on Evolutionary Computation*, pp. 182–197. doi:10.1109/4235.996017.
- [17] Deb, K., Sundar, J., Bhaskara Rao, U.N., Chaudhuri, S., 2006. Reference Point Based Multi-Objective Optimization Using Evolutionary Algorithms. Technical Report 3.
- [18] Dresig, H., Schönfeld, D., 1976a. Rechnergestützte Optimierung der Antriebs- und Gestellkraftgrößen ebene. *Koppelgetriebe-Teil 1. Mechanism and Machine Theory* 11, 363–370. doi:10.1016/0094-114X(76)90032-X.
- [19] Dresig, H., Schönfeld, S., 1976b. Rechnergestützte Optimierung der Antriebs- und Gestellkraftgrößen ebener Koppelgetriebe—Teil II. *Mechanism and Machine Theory* 11, 371–379. doi:10.1016/0094-114X(76)90033-1.
- [20] Erkaya, S., 2013. Investigation of balancing problem for a planar mechanism using genetic algorithm. *Journal of Mechanical Science and Technology* 27, 2153–2160. doi:10.1007/s12206-013-0530-z.
- [21] Farmani, M.R., Jaamiahmadhi, A., Babaie, M., 2011. Multiobjective optimization for force and moment balance of a four-bar linkage using evolutionary algorithms. *Journal of Mechanical Science and Technology* 25, 2971–2977. doi:10.1007/s12206-011-0924-8.

- [22] Farmani, M.R., Jaamolahmadi, A., 2009. Optimization of Force and Moment Balance of a Four-Bar Linkage using Multi-Objective Genetic Algorithm, in: International Mechanical Engineering Congress & Exposition, ASME International Mechanical Engineering Congress and Exposition. doi:10.1115/IMECE2009-12740.
- [23] Feng, B., Morita, N., Torii, T., 2002. A new optimization method for dynamic design of planar linkage with clearances at joints - Optimizing the mass distribution of links to reduce the change of joint forces. *Journal of Mechanical Design* 124, 68–73. doi:10.1115/1.1425393.
- [24] García-Nieto, J., López-Camacho, E., García Godoy, M.J., Nebro, A.J., Durillo, J.J., Aldana-Montes, J.F., 2016. A Study of Archiving Strategies in Multi-objective PSO for Molecular Docking, in: Dorigo, M., Birattari, M., Li, X., López-Ibáñez, M., Ohkura, K., Pincioli, C., Stützle, T. (Eds.), 10th International Conference, ANTS 2016, Proceedings, Springer, Bussels, Belgium. pp. 40–52. doi:10.1007/978-3-319-44427-7.
- [25] Holland, J.H., 1975. Adaptation in natural and artificial systems.
- [26] Hooke, R., Jeeves, T., 1961. "Direct Search" Solution of Numerical and Statistical Problems*. *Journal of the ACM (JACM)* 8-2, 212–229. doi:10.1145/321062.321069.
- [27] Li, K., Chen, R., Fu, G., Yao, X., 2019. Two-Archive Evolutionary Algorithm for Constrained Multiobjective Optimization. *IEEE Transactions on Evolutionary Computation* 23, 303–315. doi:10.1109/TEVC.2018.2855411.
- [28] Li, X., 2004. Better Spread and Convergence: Particle Swarm Multiobjective Optimization Using the Maximin Fitness Function, in: Deb, K. (Ed.), GECCO 2004, Springer-Verlag Berlin Heidelberg. pp. 117–128. doi:10.1007/978-3-540-24854-5.
- [29] Mayne, R., Sadler, J., Conte, F., George, G., 1975. Optimum Mechanism Design Combining Kinematic and Dynamic-Force Considerations. Technical Report.
- [30] Mejia-Rodríguez, R., Villarreal-Cervantes, M.G., Rodríguez-Molina, A., Pérez-Cruz, J.H., Silva-García, V.M., 2023. Evolutionary Multi-objective Design Approach for Robust Balancing of the Shaking Force, Shaking Moment, and Torque under Uncertainties: Application to Robotic Manipulators. *Mathematics* 11. doi:10.3390/math11081776.
- [31] Orvañanos-Guerrero, M.T., Acevedo, M., Sánchez, C.N., Campos-Delgado, D.U., Ghavifekr, A.A., Visconti, P., Velázquez, R., 2022. Complete Balancing of the Six-Bar Mechanism Using Fully Cartesian Coordinates and Multiobjective Differential Evolution Optimization. *Mathematics* 10. doi:10.3390/math10111830.
- [32] Orvananos-Guerrero, M.T., Sanchez, C.N., Davalos-Orozco, O., Rivera, M., Velazquez, R., Acevedo, M., 2019. Using Fully Cartesian Coordinates to Calculate the Support Reactions of Multi-Scale Mechanisms, in: Proceedings - 2018 Nanotechnology for Instrumentation and Measurement, NANOFIM 2018, Institute of Electrical and Electronics Engineers Inc. doi:10.1109/NANOFIM.2018.8688610.
- [33] Orvañanos-Guerrero, M.T., Sánchez, C.N., Rivera, M., Acevedo, M., Velázquez, R., 2019. Gradient descent-based optimization method of a four-bar mechanism using fully cartesian coordinates. *Applied Sciences (Switzerland)* 9. doi:10.3390/app9194115.
- [34] Panichella, A., 2019. An adaptive evolutionary algorithm based on non-euclidean geometry for many-objective optimization, in: GECCO 2019 - Proceedings of the 2019 Genetic and Evolutionary Computation Conference, Association for Computing Machinery, Inc. pp. 595–603. doi:10.1145/3321707.3321839.
- [35] Porter, B., Sanger, D., 1973. Synthesis of dynamically optimal four-bar linkages, in: Proc. Conf. Mechanisms, London,UK. pp. 24–28.
- [36] Price, K.V., Storn, R.M., Lampinen, J.A., 1998. Differential Evolution. A Practical Approach to Global Optimization. Springer-Verlag Berlin Heidelberg. doi:10.1007/3-540-31306-0.
- [37] Qi, N.M., Pennestri, E., 1991. Optimum balancing of four-bar linkages. *Mechanism and Machine Theory* 26, 337–348. doi:10.1016/0094-114X(91)90074-E.
- [38] Rao, S.S., Kaplan, R.L., 1986. Optimal Balancing of High-Speed Linkages Using Multiobjective Programming Techniques. *ASME. J. Mech., Trans., and Automation*, , 454–460doi:10.1115/1.3258754.
- [39] Rechenberg, I., 1978. Evolutionsstrategien, in: Schneider, B., Ranft, U. (Eds.), *Simulationsmethoden in der Medizin und Biologie*, Springer Berlin Heidelberg, Berlin, Heidelberg. pp. 83–114.
- [40] Runarsson, T.P., Yao, X., 2000. Stochastic Ranking for Constrained Evolutionary Optimization. *IEEE Transactions on Evolutionary Computation* 4, 284–294. doi:10.1109/4235.873238.
- [41] Runarsson, T.P., Yao, X., 2005. Search biases in constrained evolutionary optimization. *IEEE Transactions on Systems, Man and Cybernetics Part C: Applications and Reviews* 35, 233–243. doi:10.1109/TSMCC.2004.841906.
- [42] Seada, H., Deb, K., 2015. U-NSGA-III: A Unified Evolutionary Algorithm for Single, Multiple, and Many-Objective Optimization, in: International Conference on Evolutionary Multi-Criterion Optimization, Guimaraes, Portugal. pp. 34–49. doi:10.1007/978-3-319-15892-1.
- [43] Shang, K., Ishibuchi, H., He, L., Pang, L.M., 2020. A survey on the hypervolume indicator in evolutionary multiobjective optimization. *IEEE Transactions on Evolutionary Computation* 25, 1–20. doi:10.1109/TEVC.2020.3013290.
- [44] Shankar, B.R., Krishnamurthy, B., 2013. Optimization of Shaking Force by Discretization of Links Mass of A Planar Four Bar Mechanism. *International Journal of Engineering Research & Technology (IJERT)* 2. doi:10.17577/IJERTV2IS90150.
- [45] Srinivas, N., Deb, K., 1994. Multiobjective Optimization Using Nondominated Sorting in Genetic Algorithms. *Evolutionary Computation* 2, 221–248. doi:10.1162/evco.1994.2.3.221.
- [46] Vesikar, Y., Deb, K., Blank, J., . Reference Point Based NSGA-III for Preferred Solutions. doi:10.1109/SSCI.2018.8628819.
- [47] Walker, M.J., Haines, R.S., 1982. A study of counterweight synthesis for a 6-bar chain. *Mechanism and Machine Theory* 17, 327–334. doi:10.1016/0094-114X(82)90015-5.
- [48] Zhang, Q., Li, H., 2007. MOEA/D: A multiobjective evolutionary algorithm based on decomposition. *IEEE Transactions on Evolutionary Computation* 11, 712–731. doi:10.1109/TEVC.2007.892759.



Click here to access/download

LaTeX Source File
Mech&MachTheory - Feb2025.zip

Declaration of interests

The authors declare that they have no known competing financial interests or personal relationships that could have appeared to influence the work reported in this paper.

The authors declare the following financial interests/personal relationships which may be considered as potential competing interests: